

Radiative Mantle Experiments in JET Limiter Plasmas and Comparison to the Radiative Improved Mode in TEXTOR-94

B. Unterberg¹, M. Brix¹, R. Budny², P. Dumortier³, S.K. Erents⁴, M. von Hellermann⁵, L.D. Horton⁶, L.C. Ingesson⁵, G. Jackson⁸, A. Kallenbach⁶, K.D. Lawson⁴, A. Loarte⁷, G. Maddison⁴, G.F. Matthews⁴, A. Meigs⁴, A. Messiaen³, F. Milani⁴, P. Monier-Garbet⁹, M.F.F. Nave¹⁰, J. Ongena³, M.E. Puiatti¹¹, J. Rapp¹, J.D. Strachan², M. Tokar¹, M. Valisa¹¹, K.-D. Zastrow⁴

JET Joint Undertaking, Abingdon, Oxfordshire, UK

¹ IPP, Forschungszentrum Jülich GmbH, EURATOM Ass., D-52425 Jülich, Germany ⁺

² PPPL, Princeton University, NJ 08543 USA

³ LPP, Ass. "EURATOM- Belgian State", ERM/KMS, Brussels, Belgium ⁺

⁴ EURATOM/UKAEA Fusion Ass., Culham Science Centre, Abingdon, Oxfordshire, UK

⁵ FOM Rijnhuizen, EURATOM Ass., BE 3430 Nieuwegein, NL ⁺

⁶ Max-Planck-Institut für Plasmaphysik, EURATOM-Ass., D-85748 Garching, Germany

⁷ EFDA, close support unit, Garching, Germany

⁸ General Atomics, San Diego, CA 92186-5608, USA

⁹ Ass. EURATOM-CEA, Cadarache, France

¹⁰ Associação EURATOM/IST, CFN, Lisbon, Portugal

¹¹ Consorzio RFX, Padova, Italy

Introduction

The Radiative Improved Mode (RI-mode) [1] at the Tokamak TEXTOR-94 is obtained by seeding impurities in the plasma edge, leading not only to a possible solution for the energy exhaust by the presence of a radiating belt around the plasma, but also to improved confinement at high plasma densities (as good as in ELM-free H-mode discharges at the Greenwald density). For a possible application to a fusion reactor experiments in larger devices are necessary to investigate the influence of the machine size on the physical mechanisms leading to the improved confinement.

Experimental results

Radiative mantle experiments were performed in JET ($R_0=3.0$ m, $a=0.98$ m) using neon injection into elongated plasmas ($\kappa=1.4$) limited by the 12 poloidal carbon limiters positioned at the low field side. Auxiliary heating by neutral beam injection was applied at $P_{\text{NBI}} = 3.5 - 8.0$ MW. Toroidal field and plasma current were chosen at $B_T=2.9$ T and $I_p=1.8$ MA yielding $q_a=5$ for power handling reasons. The discharges were fuelled by the neutral beams only and reached plasma densities with respect to the Greenwald density up to $n_e/n_{\text{GW}}=0.8$. Neon was injected in short pulses with a duration of 0.5 s. Density and radiation level were rising throughout the discharge as no pumping was possible under this configuration. The fraction of radiated power $P_{\text{rad}}/P_{\text{heat}}$ was varied from 0.3 without neon injection up to 0.8

⁺ Partners in the Trilateral Euregio Cluster

with the line averaged Z_{eff} deduced from bremsstrahlung rising up to 3. The poloidal radiation distribution showed asymmetries with local maxima close to the limiter position and in the upper corner at the high field side which are thought to be caused by local carbon sources. Carbon remained the dominating impurity species even at the highest radiation levels and densities with central concentrations of C^{6+} varying from 4.5% at $P_{\text{rad}}/P_{\text{heat}} = 0.3$ and $n_e/n_{\text{GW}} = 0.4$ to 2.5% at $P_{\text{rad}}/P_{\text{heat}} = 0.8$ and $n_e/n_{\text{GW}} = 0.8$ while the concentration of Ne^{10+} rose to 1% at maximum (data from charge exchange recombination spectroscopy).

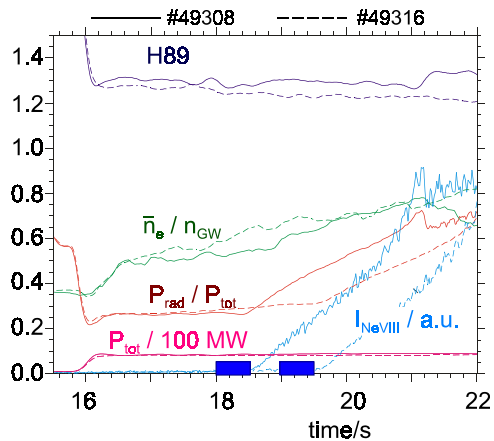


Fig. 1 Time traces of two limiter discharges with neon injection (neon puff marked with boxes)

Only marginally higher values of H89 are seen with higher radiation at a given density as shown in fig. 2a. Discharges at $P_{\text{NBI}} = 4\text{-}5 \text{ MW}$ (open boxes) perform slightly better than those at $P_{\text{NBI}} = 8\text{-}10 \text{ MW}$. No significant peaking of the density profiles could be found in these discharges (with an almost constant profile peaking factor $n_{e0}/\langle n_e \rangle = 1.4\text{-}1.6$, cf. fig. 2b). These rather limited effects of the neon injection on the global confinement are in contrast to the confinement properties of the RI-mode in TEXTOR-94 where neon injection at comparable Greenwald numbers can trigger transitions to substantially improved confinement. A characteristic feature of the RI-mode in TEXTOR-94 is indeed a pronounced peaking of the density profile ($n_{e0}/\langle n_e \rangle$ up to 2.6 at comparable q_a in TEXTOR-94[2]).

Only a moderate confinement improvement by 5-10% could be observed after the neon injection as shown in fig. 1 where time traces of the radiation level, the density with respect to the Greenwald density, the confinement time with respect to the L-mode, H89, the total heating power and the resonance line of the Li-like neon ions at the plasma edge (NeVIII at 77 nm) are shown. Two discharges are compared where one (#49316, dashed lines) had a later neon injection and can serve as a reference discharge up to $t=19.5\text{s}$.

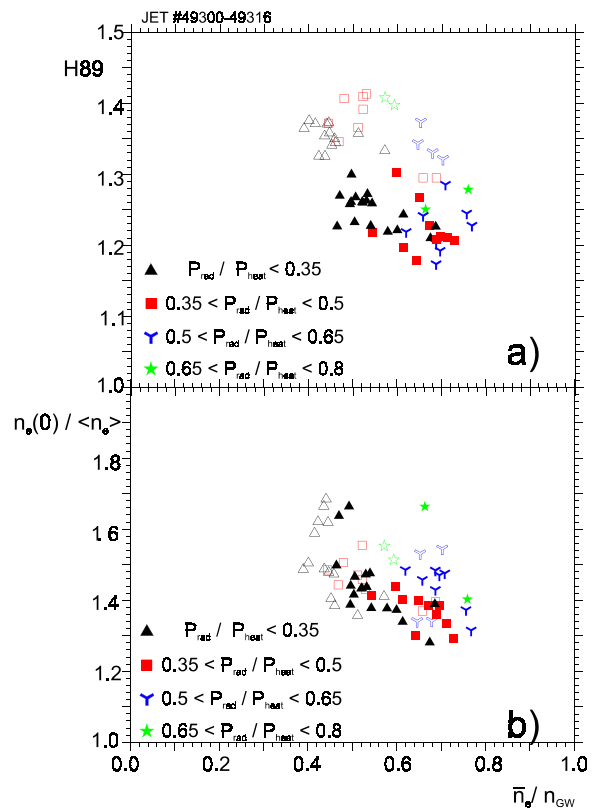


Fig. 2 Variation of a) H89 and b) the density peaking factor with the Greenwald number (open boxes $P_{\text{tot}} = 4\text{-}5 \text{ MW}$, filled boxes $P_{\text{tot}} = 8\text{-}10 \text{ MW}$)

Discussion

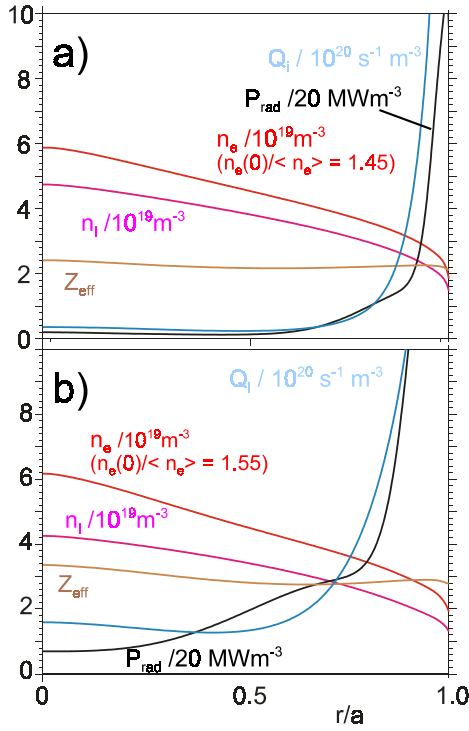


Fig. 3 Radial profiles of electron and deuteron density, ion source distribution, radiated power density and Z_{eff} calculated with the RITM code: a) JET, b) TEXTOR-94

The difference of the density profiles described above is a key issue within the comparison between JET and TEXTOR-94 as in the latter device both the increase of energy confinement and the profile peaking are attributed to the suppression of ion temperature gradient (ITG) modes in the RI-mode [3]. Therefore, the density profile of radiative mantle discharges in JET and TEXTOR-94 was modelled using the transport code RITM. In these calculations, the particle transport has been described by a shaping factor $s = -v/D \cdot a^2/r \cdot q = 0.5$ fixed for both devices (chosen to reproduce the profile shape in JET). In this modelling we take into account the differences of the radial source distributions due to the ionisation of recycled and beam fuelled neutrals in the two devices with rather different size (JET: $R_0=3.0\text{m}$, $a=0.98\text{m}$, TEXTOR-94: $R_0=1.75\text{m}$, $a=0.46\text{m}$). As seen in Fig. 3, the calculated peaking factor is comparable and the difference of the profile shapes seen in the experiments cannot be

attributed to the different source distribution directly.

To investigate the possible difference of the transport parameters a predictive description of the profile evolution successfully applied to the RI-mode at TEXTOR-94 [3] was used for JET discharge #49307. In this model, the particle flux density $\Gamma = vn - D \, dn/dr$ is given by transport coefficients v and D determined by ITG and dissipative trapped electron (DTE) modes. The diffusion coefficient D is determined by the growth rate γ_s as $D = (\gamma_s/k^2) q^2$ (k is the poloidal wave number). The ITG part has a negligible particle pinch velocity v while the DTE part has a pinch linking density and q -profile as $v/D = -d(\ln q)/dr$ (cf. [3] for details of the model). The particle conservation equation is integrated using the experimental data to determine the resulting peaking factor $p = L_T/L_n = 1/\eta$ from

$$G(p) = \Gamma(p) - 1/r \int_0^r r' S(r') dr' \equiv 0 \quad (1)$$

The function $G(p)$ is non-linear in p and characterises the possibility to have a bifurcation to a state with higher peaking. Fig. 4 shows $G(p)$ at a radial position of $r/a=0.65$ for the experimental conditions in #49307 at $t=20\text{s}$. In qualitative agreement with the experiment the model predicts a state with rather flat profiles.

The possibilities to obtain the bifurcation can be investigated by selectively changing experimental parameters. Note that p is *not* a free parameter but the result of the interplay between transport coefficients and source distribution. In TEXTOR-94 the increase of Z_{eff} has been made responsible for the initial reduction of the ITG mode allowing to reduce the maximum of $G(p)$ in between the two stable solutions until the bifurcation occurs which finally stabilises the ITG mode completely. Leaving all other parameters unchanged an increase of the

central source is most promising to reduce the local maximum of $G(p)$ below zero for JET #49307. Roughly a factor of 3 is needed with respect to the experimental one to obtain the bifurcation in this model (dashed line). On the other hand, only a further increase of Z_{eff} is not suitable for this purpose within reasonable limits as the experimental value was already high ($Z_{\text{eff}}(r/a=0.65) = 4$) and an increase by a factor of 3 would be required (Fig.4, dotted line). The effect of the higher central particle source on the profile shape is *highly non-linear* in contrast to the linear one for constant transport coefficients discussed before. However, an increase of the particle source by beam fuelling could adversely reduce the peaking due to a resulting higher temperature at the higher heating power which is unfavourable with respect to the ITG growth rate. Therefore, at the same time stronger radiation cooling inside the confined volume would be required, possibly using higher Z impurities like argon. Pellet injection with particle deposition inside $r/a=0.6$ could be an alternative or complementary scenario. The feasibility of such a density peaking has recently been shown at JET in argon seeded ELMy H-mode discharges at high density [4]. In TFTR ($R_0=2.52\text{m}$, $a=0.87\text{m}$) increased density peaking was obtained after xenon injection [5].

Summary and conclusion

Radiative mantle experiments have been made in JET using neon injection. No substantial improvement of energy confinement and density peaking are observed which are characteristic in the RI-mode at TEXTOR-94. Modelling shows that this is not a direct effect of the different central source distributions but can be attributed to differences of the transport parameters ν and D , non linearly depending on the profile shape if one assumes in the modelling that ITG and DTE driven modes are dominant.

- [1] A.M.Messiaen et al., Phys. Rev. Lettr. **77** (1996) 2487.
- [2] R. Weynants et al., Nucl. Fusion **39** (1999) 1637.
- [3] M. Tokar` et al., Phys. Rev. Lettr. **85** (2000) 895.
- [4] J.Strachan et al, to be published
- [5] K.Hill W. et al., Plasma Physics **6** (1999) 877.

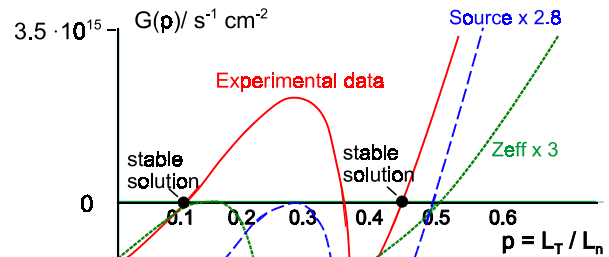


Fig. 4 Function G as a function of the peaking factor p for JET #49307 @ $r/a=0.65$, $t=20\text{s}$